Instantaneous normal mode spectra of quantum clusters

Charusita Chakravarty[a)]
Department of Chemistry, Indian Institute of Technology-Delhi, New Delhi 110016, India

Ramakrishna Ramaswamy
School of Physical Sciences, Jawaharlal Nehru University, New Delhi 110067, India

(Received 16 July 1996; accepted 23 December 1996)

The spectrum of instantaneous normal mode (INM) frequencies of finite Lennard-Jones clusters is studied as a function of the extent of quantum delocalization. Configurations are sampled from the equilibrium distribution by a Fourier path integral Monte Carlo procedure. The INM spectra, average force constants and Einstein frequencies are shown to be interesting dynamical markers for the quantum delocalization-induced cluster solid–liquid transition. Comparisons are made with INM spectra of quantum and classical Lennard-Jones liquids. The methodology used here suggests a general strategy to obtain quantal analogs of various classical dynamical quantities. © *1997 American Institute of Physics.* [S0021-9606(97)51712-0]

I. INTRODUCTION

Path integral Monte Carlo (PIMC) methods have been used extensively to simulate atomic and molecular systems to obtain canonical ensemble averages for equilibrium properties of nonfermionic systems that are, in principle, exact.[1–6] However, a computational method for simulating quantum many-body dynamics is still an elusive goal. Given this methodological bottleneck, serious efforts have been made to extract dynamical information from equilibrium Monte Carlo simulations, which have largely been fruitless except in certain special situations e.g., the study of rate processes such as electron and proton transfer.[7] Some promise of progress in this direction is held out by the instantaneous normal mode (INM) approach[8] for classical liquids and clusters. From the normal modes associated with configurations sampled from an equilibrium distribution, dynamical quantities such as the velocity autocorrelation function can be calculated with fair accuracy.[9–13] Thus the INM spectrum itself is an equilibrium property of the system that can be defined in any ensemble and from which one can hope to infer significant dynamical information.

The success of the INM approach for classical liquids suggests that it would be worthwhile to explore the consequences of treating a quantum liquid or cluster as a collection of quantum harmonic oscillators. In this article we investigate the instantaneous normal mode spectra of quantum clusters simulated through PIMC calculations. In particular, we attempt to understand the dynamical changes associated with the quantum delocalization induced cluster solid–liquid transition.[5,6]

As is by now well-known, classical clusters have several phase-dependent dynamical characteristics.[14] The largest Lyapunov exponent has a characteristic variation with energy or temperature at the cluster solid–liquid transition (CSLT).[15,16] The power spectrum of energy fluctuations in classical Lennard-Jones (LJ) clusters also shows distinctive qualitative changes during thermal melting.[15,17] These dynamical changes are reflected in classical INM spectra—the fraction of imaginary frequencies increases as the cluster becomes more liquidlike and is able to access metastable minima.[9,11]

Quantum effects have been shown to *lower* the melting and freezing temperatures of clusters.[2–5] More recently, it has been shown that quantum delocalization effects can induce a cluster solid–liquid transition (QCSLT) analogous to the thermal melting of classical clusters.[6] One would expect clusters to undergo dynamical changes during a quantum fluctuation-induced CSLT that are somewhat similar to those seen during a thermally induced CSLT. Dynamical changes associated with the QCSLT can be detected by calculating INM spectra of quantum clusters at a fixed temperature while increasing the degree of quantum delocalization by reducing the atomic mass.

A quantal instantaneous normal mode theory of liquids has recently been proposed by Cao and Voth[13] who use the path centroid probability distribution to sample liquid configurations. A variational procedure is used to obtain a set of centroid frequencies for each configuration; this includes quantum effects within a quadratic approximation. While their results for liquid Ar and Ne are encouraging, it is not clear how adequate this procedure is for systems where the quantum effects are more pronounced.

The present technique to obtain quantum INM spectra is based on the PIMC procedure, and is described in the following section, where we also briefly review the classical INM methodology. Application is made to the case of quantum clusters, and the relevant computational details are given in Sec. III. The results of our simulations are presented in Sec. IV, and this is followed by a brief summary and discussion.

II. INSTANTANEOUS NORMAL MODES—CLASSICAL AND QUANTAL

The essence of the INM concept is to approximate the total potential V at each instant as a quadratic function of the coordinates,

a)Author to whom correspondence should be addressed.

 0021-9606/97/106(13)/5564/5/$10.00

$$V(\mathbf{R}_t) \approx V(\mathbf{R}_0) - \mathbf{F}\cdot(\mathbf{R}_t - \mathbf{R}_0) + \tfrac{1}{2}(\mathbf{R}_t - \mathbf{R}_0)\cdot\mathbf{D}\cdot(\mathbf{R}_t - \mathbf{R}_0), \tag{1}$$

where $\mathbf{R}_t$ is the configuration at time t with $\mathbf{R}_0$ as the reference configuration, $\mathbf{F}$ is the instantaneous force and $\mathbf{D}$ is the Hessian, i.e., the second-derivative matrix of the many-body potential energy surface (PES), $V(\mathbf{R})$. The eigenvalues of $\mathbf{D}$, $\{\omega_1^2, \omega_2^2, \ldots, \omega_N^2\}$ are the squares of the normal mode frequencies, N being the number of degrees of freedom of the system. Thus the INM spectrum can be obtained by calculating the distribution of the frequencies along a trajectory $\mathbf{R}_t$ in a molecular dynamics simulation with Hamiltonian $H = \mathbf{P}^2/2 + V(\mathbf{R})$ where $\mathbf{P}$ is the (appropriately mass-scaled) momentum conjugate to $\mathbf{R}$. It is more common and more convenient, however, to get the INM spectra from configurations sampled from an equilibrium distribution in a MC simulation.[8]

The short-time dynamics of a liquid is expected to be governed by the dynamics of the instantaneous normal modes. The real portion of the INM spectra can be decomposed into translational, rotational, and vibrational components for a liquid. For a cluster, translational frequencies are always zero and the contribution due to the overall cluster rotations must be discarded from the INM spectra to obtain an accurate picture of intracluster dynamics.

The imaginary frequencies in INM spectra, arising from the negative eigenvalues of $\mathbf{D}$, are related to the instantaneous (real) rates of divergence in the phase space, as can be easily seen from the following. The phase space $[\mathbf{Z} \equiv (\mathbf{P}, \mathbf{R})]$ is of dimension $2N$, and the evolution of a vector in the tangent space is determined by

$$\frac{d(\delta\mathbf{Z})}{dt} = \mathscr{J}(\mathbf{Z})\,\delta\mathbf{Z}, \tag{2}$$

with

$$\mathscr{J} = \begin{pmatrix} 0 & -D \\ I & 0 \end{pmatrix}, \tag{3}$$

where $\mathbf{O}$ and $\mathbf{I}$ are null and unit matrices of order $N \times N$. Note that the Lyapunov exponents, $\lambda_1, \lambda_2, \ldots, \lambda_{2N}$ are given as[18]

$$(2^{\lambda_1}, 2^{\lambda_2}, \ldots, 2^{\lambda_{2N}}) = \lim_{n\to\infty} \left\{ \begin{array}{c} \text{magnitude of the eigenvalues of} \\ \prod_{t=0}^{n} \exp[\mathscr{J}(\mathbf{Z}_t)\,dt] \end{array} \right\}^{1/n}, \tag{4}$$

with the Jacobian matrix $\mathscr{J}$ being evaluated at n steps along a trajectory, dt being the time interval. The eigenvalues $\{\zeta_1, \zeta_2, \ldots, \zeta_{2N}\}$ of $\mathscr{J}$ are related to those of the Hessian, the ω's as

$$\zeta_{2k} = \sqrt{-\omega_k^2}, \quad \zeta_{2k-1} = -\sqrt{-\omega_k^2}, \quad k = 1,2,\ldots,N. \tag{5}$$

The positive real ζ's are local rates of divergence which measure the local instability of trajectories [$n=1$ in Eq. (4) above] which correlate with the *imaginary* INM frequencies. We note that Eq. (4) provides a method to define and evaluate the spectrum of Lyapunov exponents for a system in equilibrium, if $\mathbf{Z}_t$ (with n sufficiently large) is sampled from an equilibrium distribution.

The imaginary frequencies in INM spectra measure the extent to which the dynamics samples regions of negative curvature in the PES,[8] and these have been shown to be related to the nonzero self-diffusion constants of liquids.[10]

The normal modes associated with an equilibrium distribution for a quantum liquid or cluster can be used to construct an INM spectrum. The quantum many-body system can then be represented as a collection of quantum harmonic oscillators with frequencies distributed according to the INM spectrum. Clearly the INM spectrum for the quantum system in the limit $\hbar \to 0$ or particle mass $m \to \infty$ must coincide with the classical INM spectrum. This instance of the correspondence principle suggests a novel technique for obtaining quantal analogues of classical dynamical quantities (as for example the Lyapunov spectra) which will be explored in future work.

III. COMPUTATIONAL DETAILS

Thirteen atom Lennard-Jones clusters were studied using the Fourier path integral Monte Carlo technique which has been described in detail earlier.[4–6] For the particle masses and temperatures used in this study, identical particle exchange is unimportant. The LJ parameters were chosen to be $\epsilon = 34.2$ K and $\sigma = 2.96$ Å; this choice of ϵ and σ provides a reasonably accurate model of $(p\text{-}H_2)_{13}$ and $(o\text{-}D_2)_{13}$ clusters for particle mass m of 2 and 4 amu, respectively. The quantum LJ clusters were studied at reduced temperatures, $T^* = k_B T/\epsilon$, of 0.1, 0.15, and 0.2. The particle mass m was varied from 1645 to 1.5 amu corresponding to a variation in the de Boer parameter, $\Lambda = \hbar/\sigma\sqrt{m\epsilon}$, from 0.01 to 0.323. Each FPIMC run contained 2.5 to 5×10^6 configurations, from which 5000 configurations were sampled and the associated normal modes were determined by diagonalizing the corresponding Hessian. The three zero-frequency translational modes could be readily identified and removed. Spurious rotational modes of the cluster were removed by the procedure used in Ref. 9. Each sampled configuration was used as the starting point for a conjugate gradient minimisation to determine the nearest local minimum. The average root mean-square width of quantum paths, λ, sampled during the course of the FPIMC simulation was also monitored. As a measure of the ''average force constant'' of the cluster, the Einstein frequency, ω_E, was calculated such that

$$\omega_E^2 = \int \omega^2 p(\omega)\,d\omega, \tag{6}$$

where $p(\omega)$ is the normalised INM spectrum. ω_E can be decomposed into real, ω_R, and imaginary, ω_I, components such that

$$\omega_E^2 = (1 - F_i)\,\omega_R^2 + F_i\,\omega_I^2, \tag{7}$$

where F_i is the fraction of imaginary frequencies. It should be noted that $\omega_E^2 = \langle V'' \rangle / m(3N-6)$ where $\langle V'' \rangle$ is the MC average of the trace of the Hessian $\mathbf{D}$; thus $\langle V'' \rangle$ can be in-

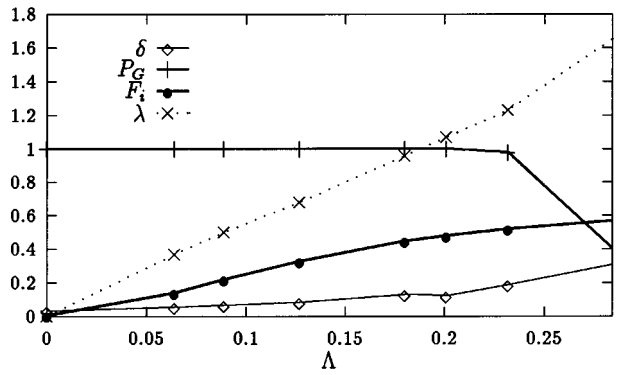

FIG. 1. Markers for the quantum cluster solid–liquid transition as a function of the de Boer parameter Λ: the probability of occupancy of the global minimum, P_G, the Lindemann index, δ, and the fraction of imaginary frequencies in the INM spectra, F_i. Also shown is the average root mean square width of quantum paths, λ, in atomic units.

terpreted as the average force constant of the cluster. The INM spectra were found to be well converged for the MC run lengths used here. Error estimates for various structural and thermodynamic quantities are discussed in Ref. 6.

While the focus of our study is primarily on cluster melting, quantum, and classical simulations of Lennard-Jones liquids were carried out at a reduced temperature $T^*=1.123$ (40 K) and reduced density $\rho^*=0.68$ for comparison with previous work.[13] The Lennard-Jones parameters were appropriate for Neon ($\epsilon=35.6$ K, $\sigma=2.75$ Å). Quantum simulations were carried out in a cubic cell of size 5.415σ with 108 atoms, for particle masses of 20 and 5 amu.

IV. RESULTS

Previous simulation results for $(LJ)_{13}$ and $(LJ)_{19}$ clusters show that the onset of melting can be characterized by the de Boer parameter value, Λ_f, for which the cluster starts to access metastable minima. Moreover, the melting transition is most abrupt and well defined in the $\Lambda=0$ and $T=0$ limits. For an $(LJ)_{13}$ cluster at $T^*=0.1$, Λ_f is approximately 0.19, corresponding to $m=4.5\pm0.5$ amu for the ϵ, σ values used here.[6] Λ_f values for $T^*=0.15$ and $T^*=0.2$ are approximately 0.152 ($m=7$ amu) and 0.104 ($m=15$ amu).

The connection between the probability of occupancy of the global minimum, P_G, and the Lindemann index, δ, has been amply demonstrated in previous work. To correlate the behavior of these CSLT indicators with the fraction of imaginary frequencies, F_i, Fig. 1 shows λ, P_G, δ, and F_i as a function of Λ at $T^*=0.1$. Classical MC results are shown for $\Lambda=0$. Notice that λ is a nearly linear function of the de Boer parameter, indicating that the latter is indeed a good index for the degree of quantum delocalization. F_i for the classical $(LJ)_{13}$ cluster at $kT/\epsilon=0.1$ is zero to within the statistical error of ±2%, once the rotational frequencies are removed. However, even for quasiclassical clusters when the cluster is unambiguously localized in the global minimum, F_i varies from 10% to 30%; this presumably reflects the ability of the cluster to sample a much wider and more anharmonic region

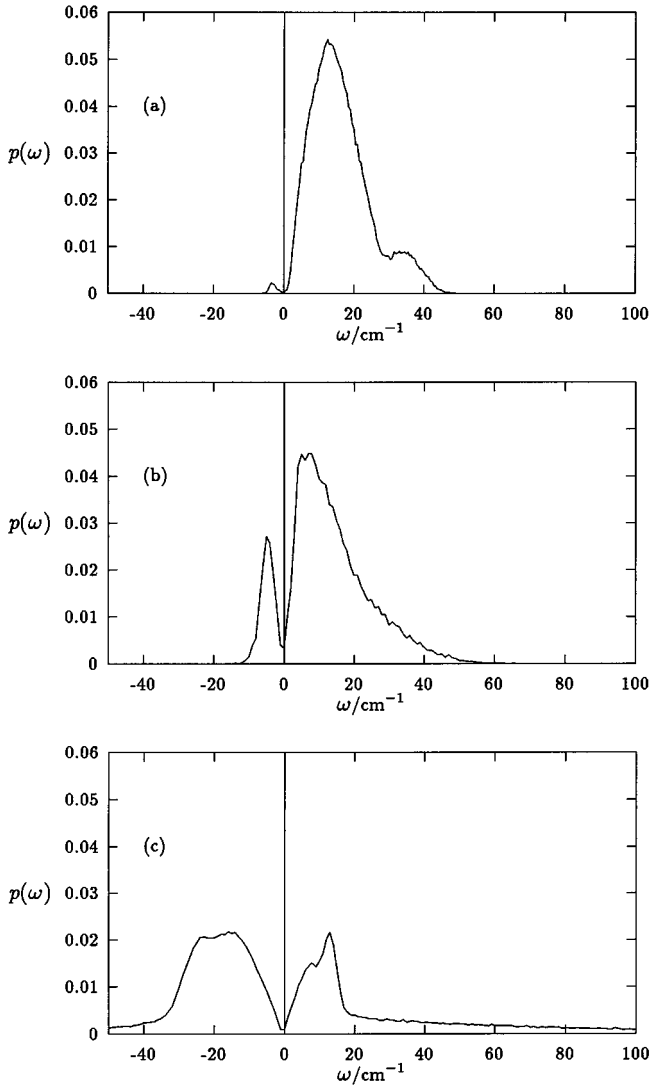

FIG. 2. INM spectra at $kT/\epsilon=0.1$ of (a) classical $(LJ)_{13}$ cluster with $m=40$ amu and 13-particle quantum $(LJ)_{13}$ clusters with particle masses (in amu) of: (b) $m=40$ ($\Lambda=0.064$) (c) $m=2$ ($\Lambda=0.284$). Frequencies are in cm^{-1} and probabilities are normalized to unity.

of the PES around the global minimum. There is no sharp increase in F_i with the onset of cluster melting when $F_i=0.57$. Similar results at $T^*=0.15$ and $T^*=0.2$ would indicate that F_i by itself does not provide a useful criterion for the CSLT. The overall variation in P_G, δ, and F_i with Λ for the QCSLT is qualitatively similar to that observed in the thermal melting of classical clusters.[6,9]

Figure 2 compares INM spectra for clusters with different degrees of quantum delocalization at $T^*=0.1$. Imaginary frequencies are plotted on the negative axis. The classical INM spectrum for $m=40$ amu at $kT/\epsilon=0.1$, shown in Fig. 2(a), has a characteristic high frequency secondary peak at ≈36 cm^{-1} which coincides with the position of the longitudinal mode peak in the phonon spectrum of the bulk solid and has virtually zero probability for imaginary frequencies. This may be compared with the quantum INM spectrum for the same value of m shown in Fig. 2(b) which has a signifi-

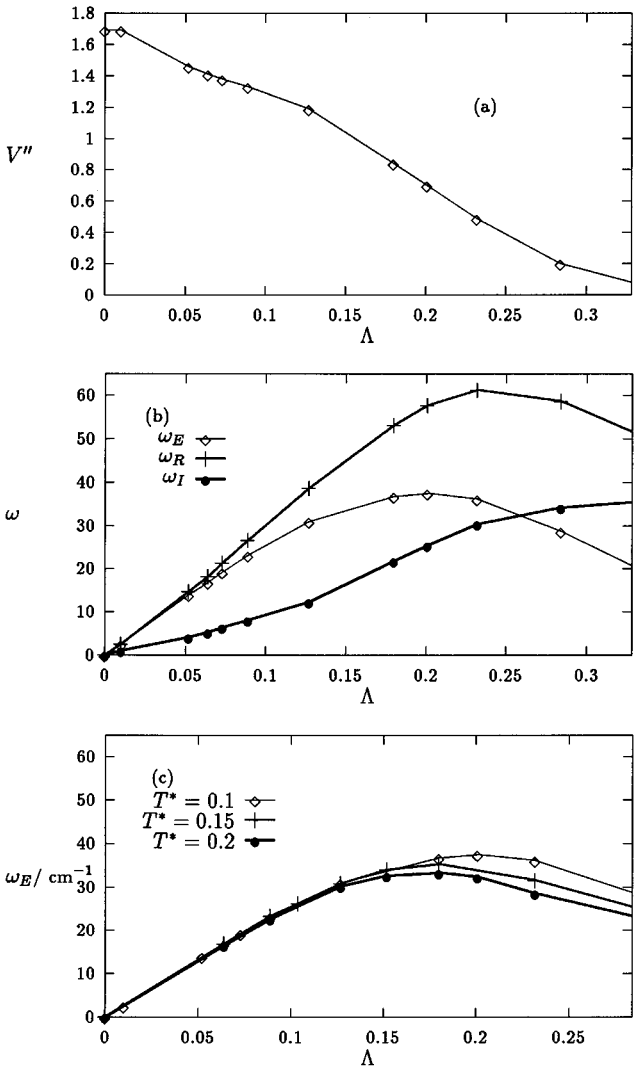

FIG. 3. (a) The average force constant, $\langle V'' \rangle / 10^{-2}$, in atomic units, as a function of Λ. (b) The Einstein frequency, ω_E (in cm^{-1}), and its real, ω_R, and imaginary components, $|\omega_I|$, are plotted as a function of Λ. All frequencies are in units of cm^{-1}. Errors in ω_E are of the order of ± 2 cm^{-1}. (c) The Einstein frequency, ω_E (in cm^{-1}), as a function of Λ for $T^*=0.1$, 0.15, and 0.2. All frequencies are in units of cm^{-1}. Errors in ω_E are of the order of ± 2 cm^{-1}.

cant peak in the imaginary portion and a broad peak in the real portion obscuring the secondary peak at 36 cm^{-1}. Decreasing particle mass enhances and broadens the peak in the imaginary frequencies and the real portion of the spectrum acquires a sharp low frequency peak and a slowly decaying high frequency tail; these features are prominent in the INM spectrum for the $m=2$ amu case shown in Fig. 2(c). This is due to both enhanced quantum delocalization and the $1/\sqrt{m}$-type dependence of the frequencies on particle mass.

Figures 3(a) and 3(b) show the averaged force constant and the Einstein frequency, respectively, as a function of Λ. From Fig. 3(a), it is obvious that the rigidity of the cluster decreases with increasing quantum delocalization and the rate of decrease is enhanced with the occupancy of metastable minima. The Einstein frequency, ω_E, has a mass-dependence in the classical limit; since in the present work the $\Lambda \to \infty$ limit coincides with the $m \to \infty$ limit, the classical value of ω_E is shown as zero. In this context, for purely classical clusters, ω_E would have a linear dependence on Λ (or on $1/\sqrt{m}$). For a given value of particle mass, introduction of quantum effects lowers ω_E from its classical value because of decreasing cluster rigidity. The $\omega_E(\Lambda)$ curve shows a clear maximum very close to Λ_f. To understand the shape of the $\omega_E(\Lambda)$ curve, the real, ω_R, and imaginary, ω_I, components are also shown in Fig. 3(b). The magnitude of both ω_R and ω_I increases with Λ. The increase in $|\omega_I|$ must originate from enhanced sampling of low-frequency anharmonic regions. ω_R as a function of Λ is virtually identical to the classical Einstein frequency until $\Lambda=\Lambda_f$; therefore the increase in ω_R can be largely attributed to a simple mass effect. The high proportion of barrier crossing motions in the liquidlike cluster for $\Lambda > \Lambda_f$ results in decreasing cluster rigidity, a levelling off in the $\omega_R(\Lambda)$ value and a relatively rapid rise of the $\omega_I(\Lambda)$ curve. Alternatively, we can explain the maximum in ω_E as a consequence of two competing effects: (a) an increase in ω_E with decreasing m or increasing Λ due to a $1/\sqrt{m}$ dependence of the frequencies and (b) a decrease in the average force constant of the cluster with increasing quantum delocalization. Once the occupancy of the metastable minima becomes significant, the second effect becomes the dominant one and the slope of the $\omega(\Lambda)$ curve becomes negative. However, once P_G becomes very nearly zero and the cluster is in a liquidlike state, the slope of the ω_E curve may change or become nearly zero. Figure 3(c) compares the $\omega_E(\Lambda)$ curves at $T^*=0.1$, 0.15, and 0.2. The maximum in the $\omega_E(\Lambda)$ is most clearly marked at $T^*=0.1$ and broadens with increasing temperature. This is to be expected since thermal fluctuations will tend to make the onset of the QCSLT less abrupt. However, the qualitative similarity in the shape of the three curves is notable.

Figure 4 shows the classical INM spectra for liquid neon at $T^*=1.123$ and $\rho^*=0.68$ and compares it with the quantum INM spectra for $m=20$ (neon) and $m=5$ amu. The quantum and classical INM spectra for liquid Ne at this temperature, shown in Fig. 4(a), are virtually identical. When m is reduced to 5 amu [see Fig. 4(b)], quantum effects result in a slight enhancement of the imaginary portion of the spectrum, as expected on the basis of our results for quantum clusters. The fraction of imaginary frequencies (F_i) for the quantum liquid is 0.38, as compared to 0.35 for the classical system. Our results are also consistent with the well-known deviations from the classical principle of corresponding states due to quantum effects.[19] For example, Ar has a melting point of 83.8 K ($T^*=0.702$ for $\epsilon=119.4$ K). From the principle of corresponding states, the melting point of Neon is predicted to be 24.98 K for $\epsilon=35.6$ K. This is in good accord with the actual melting point of Neon, namely 24.5 K, confirming that quantum effects in liquid Neon near the melting temperature are small. As mentioned in Sec. III, the p-H_2 system can be treated as a psuedo-atomic system at low temperature with $\epsilon=34.2$ K and $\sigma=2.96$ K. The predicted value of the melting temperature for p-H_2 would then be 24 K which is much higher than the experimental value of 13.9 K. This indicates

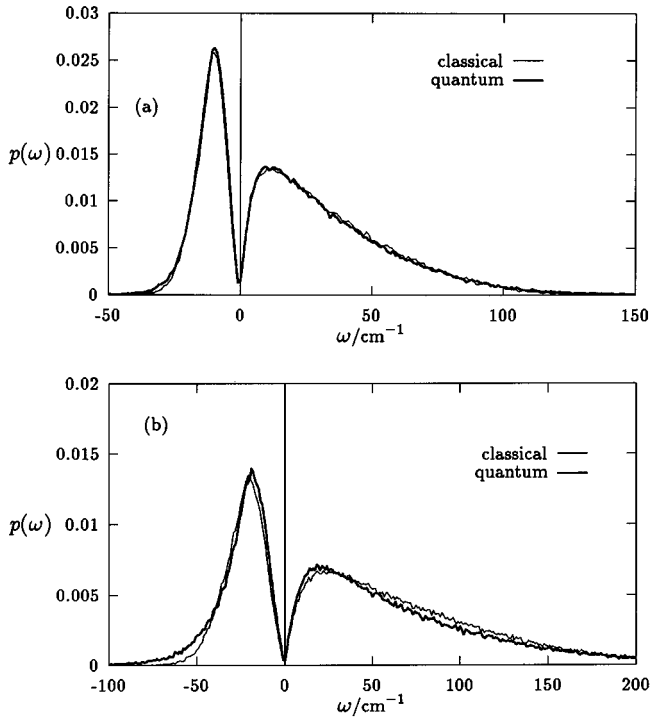

FIG. 4. Classical and quantum INM spectra for a Lennard-Jones liquid at $T^*=1.123$ and $\rho^*=0.68$ for particle mass of (a) 20 amu and (b) 5 amu. Frequencies are in cm^{-1} and probabilities are normalized to unity.

that enhanced quantum effects will result in a promotion of spatial delocalization and a consequent lowering of melting temperature; an expectation that is unequivocally supported by our simulation studies as well as previous work.[1–6]

A comparison should be made at this point with the results of Cao and Voth,[13] whose calculations show that quantum effects *reduce* the fraction of imaginary frequencies in the INM spectra of liquid neon. In light of the above discussion, this conclusion appears counterintuitive and suggests that the correspondence between observables calculated within the centroid path formalism and within the PIMC framework needs to be explored further. We should point out that PIMC methods have been extensively tested, in many cases against experimental results, for a variety of quantum liquid and solid systems. For quasiclassical systems like Neon, there is every reason to expect quantitative accuracy (within the limits of the accuracy of the pair potential and statistical error) from PIMC simulations.

V. CONCLUSIONS

We have presented a technique for obtaining quantal INM spectra for clusters using PIMC simulations. Our study shows that the dynamical changes accompanying the QCSLT have characteristic signatures in the INM spectrum. The INM spectra acquire an increasing fraction of imaginary frequencies as the QCSLT progresses; simultaneously, the lower mass results in an enhanced high frequency tail. The overall cluster rigidity, as measured by the thermally averaged trace of the Hessian, decreases with increasing quantum delocalization. The Einstein frequency, ω_E, as a function of the particle mass, shows a maximum for parameter values corresponding to the onset of cluster melting.

Several studies in the literature have shown the qualitative similarity in behavior of various structural, thermodynamic and dynamical observables for magic number quantum and classical Lennard-Jones (or similar pair-potential) clusters of different sizes. We therefore expect the conclusions of this study, which are based on both cluster as well as liquid-state simulations, to have much wider validity. Moreover, the methodology used to extract quantum INM spectra may prove very useful in defining quantal analogues of other classical dynamical quantities of interest.

ACKNOWLEDGMENTS

C.C. would like to thank the Computer Science and Engineering Department, I. I. T-Delhi, for the use of their computational facilities and the Department of Science and Technology for financial assistance (Grant IITD/IRD/RP-112/95). R.R. acknowledges the support of the Department of Science and Technology (Grant SPS/MO-5/92) and the CSIR, India.

[1] K. E. Schmidt and D. M. Ceperley, in *The Monte Carlo Method in Condensed Matter Physics*, edited by K. Binder (Springer–Verlag, Berlin, 1992); D. M. Ceperley, Rev. Mod. Phys. **67**, 279 (1995).
[2] J. D. Doll, D. L. Freeman, and T. L. Beck, Adv. Chem. Phys. **78**, 61 (1990); D. M. Leitner, J. D. Doll, and R. M. Whitnell, J. Chem. Phys. **94**, 6644 (1991); R. W. Rick, D. M. Leitner, J. D. Doll, D. L. Freeman, and D. D. Frantz, *ibid*. **95**, 6658 (1991).
[3] D. Scharf, M. L. Klein, and G. J. Martyna, J. Chem. Phys. **97**, 3590 (1992); P. Sindzingre, D. M. Ceperley, and M. L. Klein, Phys. Rev. Lett. **67**, 1871 (1991); D. Scharf, G. J. Martyna, and M. L. Klein, Chem. Phys. Lett. **197**, 231 (1992).
[4] C. Chakravarty, J. Chem. Phys. **102**, 956 (1995).
[5] C. Chakravarty, Mol. Phys. **84**, 845 (1995).
[6] C. Chakravarty, J. Chem. Phys. **103**, 10663 (1995).
[7] G. A. Voth, D. Chandler, and W. H. Miller, J. Chem. Phys. **91**, 7749 (1989); M. Marchi and D. Chandler, *ibid*. **95**, 889 (1991).
[8] R. M. Stratt, Acc. Chem. Res. **28**, 201 (1995).
[9] J. E. Adams and R. M. Stratt, J. Chem. Phys. **93**, 1358, 1332, 1632 (1990).
[10] B. Madan and T. Keyes, J. Chem. Phys. **98**, 3342 (1994).
[11] V. Buch, J. Chem. Phys. **93**, 2631 (1990).
[12] M. Buchner, B. M. Ladanyi, and R. M. Stratt, J. Chem. Phys. **97**, 8522 (1992).
[13] J. Cao and G. A. Voth, J. Chem. Phys. **101**, 6184 (1994).
[14] R. S. Berry, J. Phys. Chem. **98**, 6910 (1994).
[15] S. K. Nayak, R. Ramaswamy, and C. Chakravarty, Phys. Rev. E. **51**, 3376 (1995); S. K. Nayak, R. Ramaswamy, and C. Chakravarty, Phys. Rev. Lett. **74**, 4181 (1995).
[16] P. Butera and G. Caravati, Phys. Rev. A **36**, 962 (1987); A. Bonasera, V. Latora, and A. Rapisarda, Phys. Rev. Lett. **75**, 3434 (1995); Y. Yamaguchi, preprint LANL/chao-dyn 9602002, 1996.
[17] S. K. Nayak and R. Ramaswamy, Proc. Indian Acad. Sci. (Chem. Sci) **106**, 521 (1994); S. K. Nayak and R. Ramaswamy J. Phys. Chem. **98**, 9260 (1994).
[18] J. P. Eckmann and D. Ruelle, Rev. Mod. Phys. **57**, 617 (1985); M. Pettini, Phys. Rev. E. **47**, 828 (1992).
[19] M. Toda, R. Kubo, and N. Saito, *Statistical Physics I: Equilibrium Statistical Mechanics* (Springer, Berlin, 1992).